Numerical study of the detailed structure of the ion resonance cone

G. Bonhomme, Th. Pierre, and G. Leclert
Laboratoire de Physique des Milieux Ionisés URA 835 du CNRS, Université Henri Poincaré, Nancy I, Boîte Postale 239, F-54506 Vandoeuvre Cedex, France
(Received 4 April 1994)

The detailed structure of the ion resonance cone radiated by a point source antenna in a warm magnetized plasma at a frequency lower than the ion cyclotron frequency is numerically investigated. Aside from the existence of the previously reported ion resonance cone, an axial modulation of the amplitude of the radiated potential in the direction parallel to the magnetic field is shown to be always present. The modulation length is related to the frequency value and to the electron to ion temperature ratio through the peculiar shape of the dispersion surface. This result, together with the fact that the constant-phase conical surfaces have an aperture angle very different from the resonance cone angle, can provide an effective way to estimate the ion temperature.

PACS number(s): 52.35.Fp, 52.40.Fd

I. INTRODUCTION

The radiation of a point source antenna in a warm collisionless plasma immersed in a magnetic field has been extensively studied during the past 20 years and is often related to the resonance cone phenomenon. For instance, see the Clemmow-Mullaly-Allis (CMA) diagram given by Stix [1] and Walker [2] or Ohnuma [3] for a review paper. Considering the propagation of some electrostatic and electromagnetic waves, the magnetic field induces a strong anisotropy of the medium leading to the existence of a narrow angle of radiation from the antenna at certain frequencies. In the high frequency range, this happens near the electron plasma and cyclotron frequency, leading to the upper hybrid and lower hybrid resonance cones [4,5]. The electric field is greatly enhanced on these conical surfaces whose axis is along the direction of the magnetic field and whose apex is on the emitting point. The same phenomenon is appearing for the ion waves below the ion cyclotron frequency in a warm magnetized plasma [6,7]: a range of low damped wave vectors is determining a mean group velocity angle dependent on the vicinity of the frequency to the ion cyclotron frequency. The energy is then radiated only along or inside a cone whose axis is parallel to the magnetic field. Contrary to the now well documented electron resonance cones, which are commonly used as a diagnostic tool in laboratory plasmas as well as for the ionospheric measurements, less attention has been paid to the case of the low frequency resonance cones. Considering the ion waves, this phenomenon has seldom been observed experimentally [8,9] in not very suitable conditions, often very close to the antenna and in a plasma column of a rather small diameter compared to the ion gyroradius. We are presenting here a numerical two-dimensional study of the radiated potential near the point source antenna below the ion cyclotron frequency. The results are discussed in terms of intrinsic diffraction in relation with a model previously introduced in the case of the electron modes [10,11].

II. THE RADIATED POTENTIAL

The dispersion relation of electrostatic modes in the warm magnetized plasma can be expressed as

$$\varepsilon(\omega,k_\perp,k_\parallel)\equiv 1+\frac{1}{k^2\lambda_{De}^2}\left[1+\sum_{-\infty}^{+\infty}I_n(\lambda_e)e^{-\lambda_e}\zeta_{0e}Z(\zeta_{ne})\right]+\frac{1}{k^2\lambda_{Di}^2}\left[1+\sum_{-\infty}^{+\infty}I_n(\lambda_i)e^{-\lambda_i}\zeta_{0i}Z(\zeta_{ni})\right]=0, \tag{1}$$

where $\lambda_e=\frac{1}{2}k_\perp^2r_{Le}^2$; $\lambda_i=\frac{1}{2}k_\perp^2r_{Li}^2$; $\varsigma_{ne}=(\omega+n\omega_{ce})/k_\parallel V_{Te}$; $\varsigma_{ni}=(\omega+n\omega_{ci})/k_\parallel V_{Ti}$; and r_{Le}, r_{Li} are the electron and ion Larmor radii; V_{Te}, V_{Ti} are the electron and ion thermal velocities; λ_{De}, λ_{Di} are the electron and ion Debye lengths and ω_{ce}, ω_{ci} are the electron and ion cyclotron angular frequencies.

The corresponding dispersion branches in the low frequency range are related to the pure ion Berstein wave (PIBW) when the wave vector is exactly perpendicular to the magnetic field, to the neutralized ion Berstein wave (NIBW) when the wave vector departs from the exact perpendicular direction and to the electrostatic ion cyclotron mode, i.e., the ion acoustic wave (ESICW).

For a high value of the T_e/T_i ratio, the inequality $V_{Ti}\ll\omega/k_\parallel\ll V_{Te}$ holds. In this limit, electrons are fully magnetized, ions are cold, and the following approximate dispersion relation (see, for example, Kuehl [6]) can be derived :

$$k_\parallel^2\lambda_{De}^2\left(\omega_{pi}^2-\omega^2\right)+k_\perp^2\lambda_{De}^2\left(\frac{\omega_{pi}^2}{\omega^2-\omega_{ci}^2}-1\right)\omega^2-\omega^2=0. \tag{2}$$

This relation will be useful in the next section when discussing some limiting cases.

The display of the dispersion surfaces would show that strong directional effects are present in each case due to the complicated evolution of the dispersion curves with changing the angle of the wave vector. On each branch, the radiated potential can be calculated using Kuehl's method [12]:

$$\Phi(r) = \frac{i}{4\pi\varepsilon_0} \sum_m \int_0^{+\infty} dk_\parallel \frac{H_0^{(1)}(k_{\perp m} r_\perp) \cos(k_\parallel r_\parallel)}{D'_m(k_\parallel)}, \quad (3)$$

where

$$D'_m(k_\parallel) = \left.\frac{\partial D}{\partial k_\perp^2}\right|_{k_\perp = k_{\perp m}(k_\parallel)}$$

$$\text{with} \qquad D = (k_\perp^2 + k_\parallel^2)\varepsilon(\omega, k_\perp, k_\parallel) \quad (4)$$

and $H_0^{(1)}$ is the first kind zeroth order Hankel function.

III. NUMERICAL RESULTS

Keeping only the least damped root of the dispersion equation of the ESICW below the ion cyclotron frequency, the major parameter determining the accuracy of the calculation is the domain of integration on the $k_\parallel$ axis. This domain has to be truncated once the damping coefficient $\mathrm{Im}(k_\perp)/|k|$ becomes large enough (typically 0.2) with no longer a significant contribution to the summation. The accuracy of the calculation has also been checked by choosing different $k_\parallel$ steps. Moreover, special care is taken in evaluating the Hankel function when the argument becomes very low, i.e., at very low angles along the magnetic field.

Previous numerical investigations on electron resonance cones [13] have pointed out that the distance to the emitter has to be large enough in order to obtain a clear and somewhat asymptotic value of the potential pattern. Such a large distance is more easily obtained, as for experiments, by choosing a low mass gas. For the sake of simplicity owing to their single ionization state, helium ions have been considered.

A typical index surface obtained with helium at $\omega_{pi}/\omega_{ci} = 30$, $\omega/\omega_{ci} = 0.6$, and a temperature ratio $\Theta = T_e/T_i = 50$ is displayed in Fig. 1. It is worth noting that the damping is negligible only on a rather restricted part of the $k_\parallel$ axis. The approximate dispersion relation of the preceding section gives the $k_\parallel$ value at which the real part of $k_\perp$ decreases abruptly to zero. This value is in fact close to the solution of the dispersion relation of the ion acoustic mode propagating along the B field, as shown by direct inspection of Eq. (1) . At finite values of the Θ ratio, only a numerical solution is possible, because the argument of the plasma dispersion function becomes of the order of unity. In any case for low values of Θ (say, $\Theta = T_e/T_i < 10$) the ion modes are strongly damped, so that the amplitude is significant only near the source.

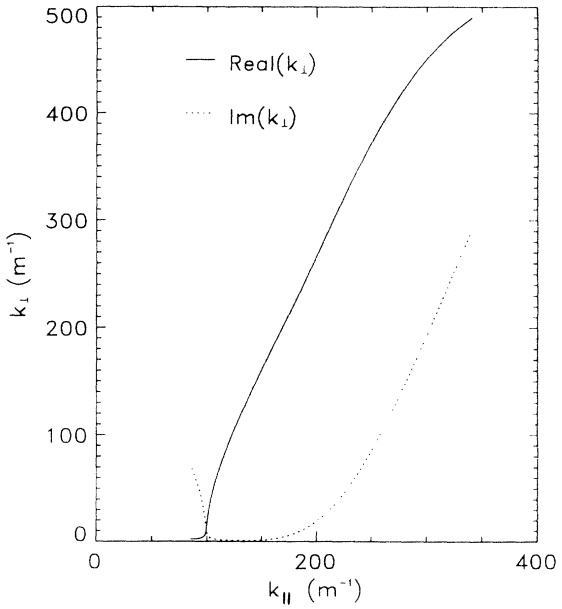

FIG. 1. Index surface of the ion cyclotron wave below the ion cyclotron frequency (full line). The damping (dashed line) is negligible only on a restricted part of the $k_\parallel$ axis. The parameters are $\omega_{pi}/\omega_{ci} = 30$, $\omega/\omega_{ci} = 0.6$, and a temperature ratio $\Theta = T_e/T_i = 50$.

As usual, the direction of the group velocity, i.e., the direction of propagation of energy, is perpendicular to the index curve as long as the damping is negligible. For the modes under consideration, because of the curvature of the index curve in the restricted range of the $k_\parallel$ axis with low damping, the group velocity direction fills roughly the interior of the resonance cone angle. This results in a broadening of the resonance cone itself and in the propagation of energy along the z axis.

The mean group velocity on this part, whose direction is perpendicular to the index surface, determines the direction of propagation of the energy, i.e., the cone angle. The two-dimensional calculation of the radiated potential is then performed using Kuehl's method. The map depicted in Fig. 2 shows the amplitude of the potential calculated in front of the point source antenna up to 15 cm in the axial direction and 6 cm in the radial direction at a frequency $\omega = 0.6\omega_{ci}$ and $\Theta = T_e/T_i = 50$. The resonance cone is easily seen with a well-defined aperture angle. Moreover, a strong axial potential modulation is observed in the axial direction. The physical reality of this phenomenon has been checked by changing the various numerical integration parameters. It can be easily understood that the restriction of the calculation of the radiated potential at two different distances around the emitter can be misleading and give two very different cone angles. The complicated potential structure at a small angle interacting with the ion resonance cone itself leads to the necessity of the two-dimensional study reported here.

Figure 3 shows that this unexpected axial modulation depends on the ion temperature: the modulation length is slightly decreasing with increasing the T_e/T_i ratio. The

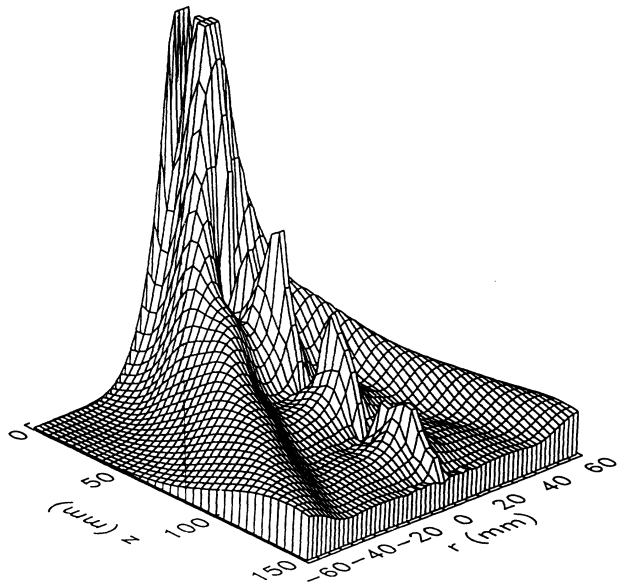

FIG. 2. Two-dimensional map of the radiated potential in the half-plane in front of the point source antenna ($\omega/\omega_{ci} = 0.6, \Theta = T_e/T_i = 50$). The magnetic field direction is along the z axis and the point source antenna is located at ($r = 0, z = 0$). The amplitude is maximum along the ion resonance cone.

modulation equivalent wave number is nearly equal to the $k_\parallel$ value for which $k_\perp$ undergoes a transition from a large imaginary value (large damping) to a large real value (small damping). One expects that the modulation length of the potential amplitude is roughly half the wavelength corresponding to this value of $k_\parallel$. At $\omega = 0.6\omega_{ci}$, one finds (Fig. 1) $k_\parallel = 100$ m $^{-1}$, giving an associated wavelength $\pi/k_\parallel \approx 3$ cm. The modulation length appearing on the computed potential is also $\lambda^* \approx 3.5$ cm in that case. In fact, the modulation length is always slightly greater than $\pi/k_\parallel$ because lower wave numbers are still relatively undamped and contribute to the potential. For example, at $\Theta = 10$, $\pi/k_\parallel \approx 4.6$ cm, whereas one finds $\lambda^* \approx 4.7$ cm.

This phenomenon has been checked at different frequencies below ω_{ci}. Very similar results have been obtained by de Feraudy and Lembège [10] for electron resonance cones and have led to their intrinsic diffraction model. In the frame of this description, the radiated potential is shown to be spatially modulated in the same way as the optical intensity behind a screen with sharp edges. We think that this model can be applied to the ion waves radiated by a point source antenna below the cyclotron frequency, due to the existence of this abrupt increase at some particular $k_\parallel$ value. But in this case, due to the sharp decrease of the real part of $k_\perp$, there exists a well-defined value of $k_\parallel$, say $k_{\parallel 0}$, for which $|k_\perp|$ is small. This results in a peculiar behavior on the z axis: according to Eq. (3) and to the behavior of the Hankel function $H_0^{(1)}$, the amplitude must be nonzero and modulated at the wavelength λ^* corresponding to $k_{\parallel 0}$ in the vicinity of the z axis. This modulation can in principle be seen at large z, although it will eventually damp out.

Aside from the evolution of the modulation length mentioned above, it is worth noting that the contrast of the diffraction pattern is rapidly changing. It is more pronounced at higher ion temperature, reaching 100% at $\Theta = 10$. A careful interpretation during the ion resonance cone measurements is then necessary in order to obtain an unambiguous determination of the cone angle, especially when it has a small value, i.e., at a frequency lower than half the ion cyclotron frequency.

Another important point for the characterization of the ion resonance cone is the comparison of the angle between the wave surfaces and the magnetic field direction and

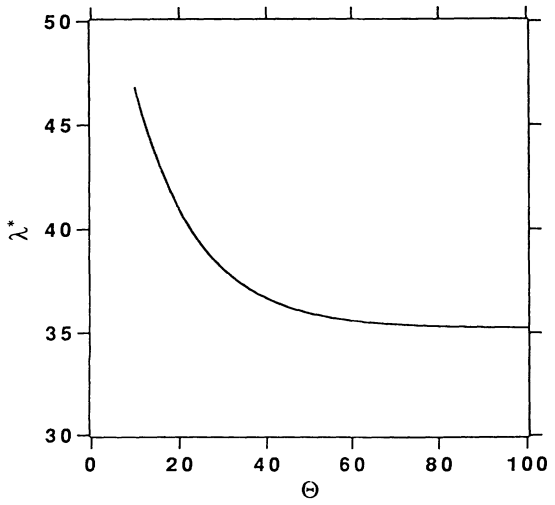

FIG. 3. Evolution of the axial modulation length λ^* as a function of the temperature ratio Θ.

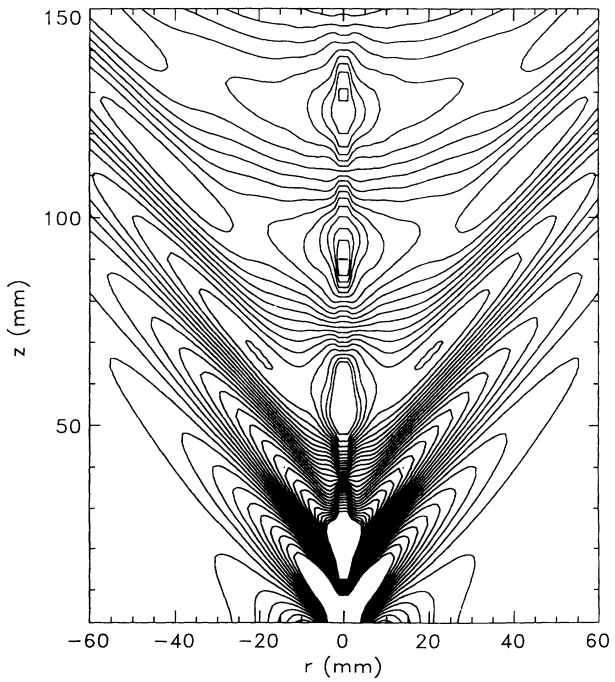

FIG. 4. Pattern of the interference map exhibiting the finite angle of the wave fronts with respect to the B-field axis.

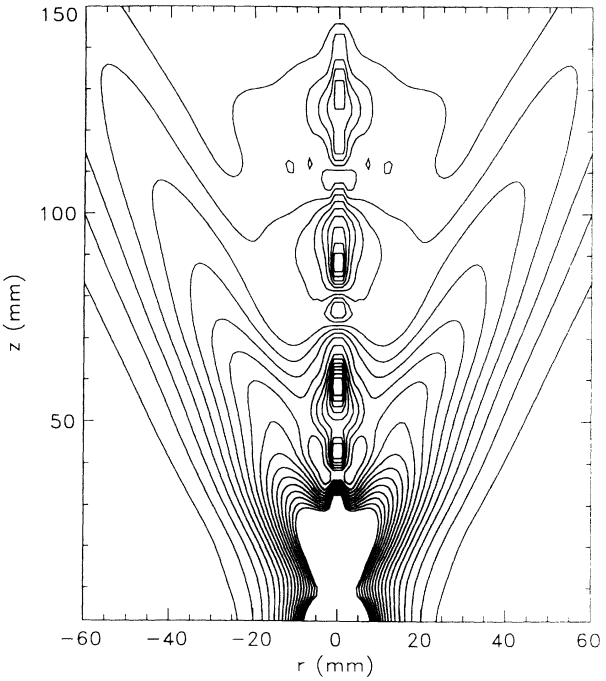

FIG. 5. Constant amplitude contour plot of the radiated potential in the same case. The cone angle is clearly different from the angle of the conical wave surfaces.

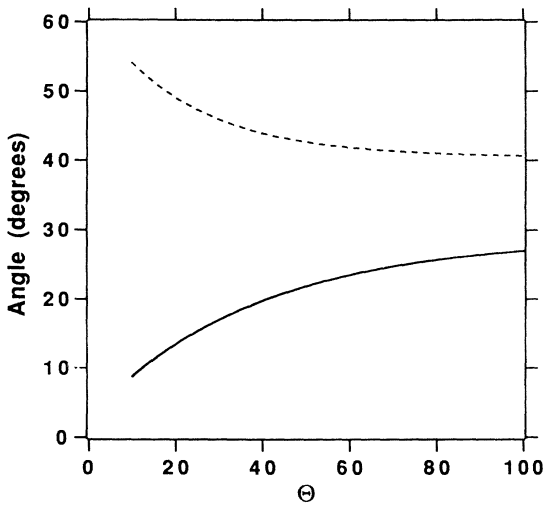

FIG. 6. Dependence of the cone angle (solid line) and of the wave surface angle (dashed line) on the ion temperature ratio.

the angle of the cone itself. In fact, due to the thermal effects, these angles are very different in most cases. This is completely different in the case of the electron modes: in that case, the constant phase and maximum amplitude cones have exactly the same aperture angle. That is, the electron resonance cone is an equiphase structure. In order to exhibit clearly this different behavior in the case of the ion resonance cones, an interference map has been calculated by mixing the radiated potential with a high level reference potential at the same frequency. This is indeed the way the experiment will have to be done, in order to record the wave fronts. Figure 4 shows the pattern of the wave fronts appearing after the mixing with the reference signal and Fig. 5 displays the lines of constant amplitude in that exact case without mixing. In the proposed experiment, using a network analyzer, both records are made simultaneously, but the existence of parasitic couplings between the emitter and the receiver leads to a much more reliable ion temperature estimation from the phase measurement.

The phase surfaces appearing in Fig. 4 are conical surfaces with an aperture angle (40°) clearly greater than the angle of the resonance cone (23°). Once again, the complicated structure along the z axis is due to the intrinsic diffraction effects interfering with the wave fronts at a modulation length clearly shorter than the distance between the wave fronts. It is interesting to compare in Fig. 6 the evolution of the cone angle (bold line) and of the angle of the conical wave surfaces (dashed line) as a function of the ion temperature. The difference between these two values is higher at high ion temperature and remains not negligible at low values of the ion temperature. This phenomenon could be a good experimental test for the estimate of the ion temperature.

IV. CONCLUSIONS

These numerical results show that the detailed structure of the ion resonance cone has to be taken into account in the experiments. The existence of an axial modulation of the radiated potential can lead to a complicated record during interferographic measurements. On the other hand, a careful analysis of this new phenomenon can lead to an easy determination of the ion temperature which is a parameter rather difficult to measure using conventional gridded probes. For instance, the modulation length is decreasing at a higher temperature ratio. The relative amplitude of this diffraction phenomenon is also enhanced at low ion temperature. Moreover, the difference in the angles of the cone itself and of the conical wave surfaces is a good test for the estimate of the ion temperature.

[1] T.H. Stix, in *The Theory of Plasma Waves* (McGraw-Hill, New York, 1962).
[2] A.D.M. Walker, J. Plasma Phys. **17**, 467 (1977).
[3] T. Ohnuma, IEEE Trans. Plasma Sci. **6**, 464 (1978).
[4] R.K. Fisher and. R.W. Gould, Phys. Fluids **14**, 857 (1971).
[5] Th. Pierre and G. Leclert, Plasma Phys. Controlled Fusion **31**, 371 (1989).

[6] H.H. Kuehl, Phys. Fluids **17,** 1636 (1974).
[7] K.H. Burrel, Phys. Fluids **18,** 897 (1975).
[8] T. Ohnuma, T. Kuwabara, S. Adashi, and K. Shibata, Phys. Rev. Lett. **37,** 206 (1976).
[9] P. Bellan, Phys. Rev. Lett. **32,** 903 (1976).
[10] H. de Feraudy and B. Lembège, Phys. Fluids **28,** 2755 (1985).
[11] H. de Feraudy, Phys. Fluids **29,** 122 (1986).
[12] H.H. Kuehl, Phys. Fluids **16,** 1311 (1973).
[13] B. Lembège, Phys. Fluids **27,** 412 (1984).

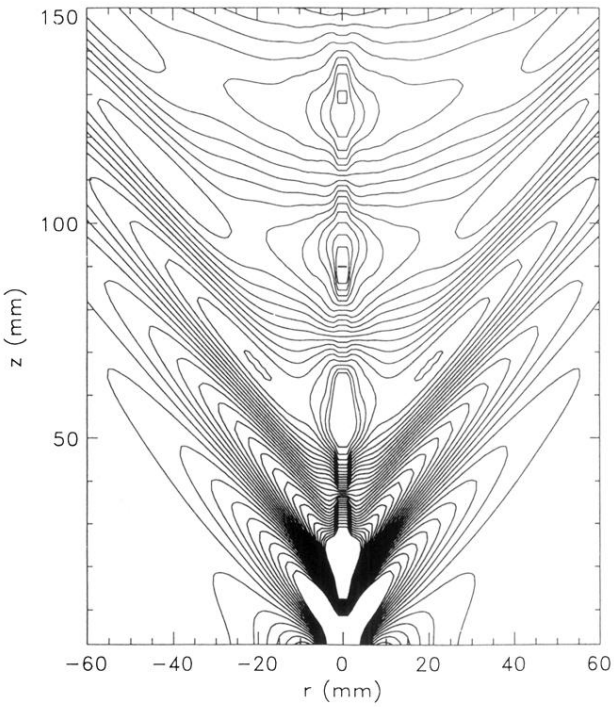

FIG. 4. Pattern of the interference map exhibiting the finite angle of the wave fronts with respect to the B-field axis.

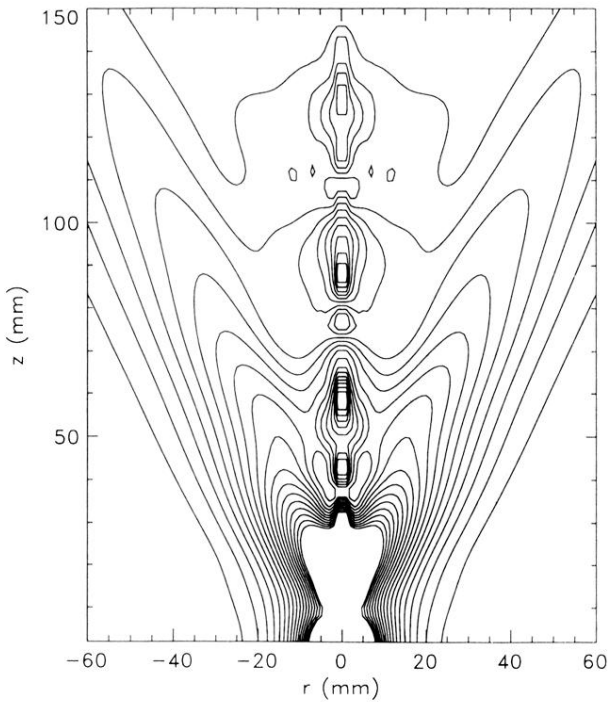

FIG. 5. Constant amplitude contour plot of the radiated potential in the same case. The cone angle is clearly different from the angle of the conical wave surfaces.